DYNAMIC SNAP-THROUGH OF A SIMPLE VISCOELASTIC TRUSS*

BY

W. NACHBAR AND N. C. HUANG

University of California, San Diego

Abstract. In order to understand the behavior of shallow structures in dynamic snap-through or buckling, a detailed study has been made for a plane, viscoelastic, three-hinged truss with a concentrated mass at the central hinge, and with a normal load of constant magnitude applied suddenly at this hinge. The dynamic buckling criterion is found to correspond to values of the parameters for which the solution goes into the saddle point of a two-dimensional autonomous system. It is shown that another dynamic buckling criterion, based upon the asymptotic behavior of solutions in time, can give incorrect results in certain cases. Two methods to compute buckling loads are investigated with the aid of a phase plane diagram and potential curves. Approximations to the buckling load, including an upper bound, are computed by means of an energy integral method. The exact buckling loads are computed by numerical integration of the governing differential equation.

1. Introduction. In recent years, much attention has been given to problems of the dynamic buckling of structures on account of their importance in engineering. In this paper, we shall be concerned with a basic study of dynamic snap-through behavior by considering a plane three-hinged simple truss with a concentrated mass at the central hinge as shown in Fig. 1. The material of the structure is assumed to be viscoelastic with a stress-strain relation represented by the Voigt (Kelvin) model. A concentrated load is suddenly applied to the central hinge and is maintained thereafter. The purpose of this paper is to find the critical magnitude at the load for snap-through under various conditions.

The static snap-through problem of the same structure was investigated by Mises [1] for the elastic case and by Hult [2] and Huang [3] for the linear and nonlinear viscoelastic cases. In the two latter cases, the viscoelastic materials are assumed to be capable of flow without limit, and snap-through always occurs. The Voigt solids behave differently. The deformation of a Voigt solid asymptotically approaches a delayed elastic equilibrium state, and snap-through of the structure will not occur if the magnitude of load is below a certain critical value.

In order to achieve a thorough understanding of this problem, we shall employ the aid of both the phase plane diagram and the potential curves in our analysis. Two methods are used: the energy integral method and the direct method. The direct method is based upon the numerical solution of the governing differential equation and initial conditions. The energy method is an extension to dissipative systems of a method previously applied to elastic structures; in it the buckling load is determined, without first finding the explicit solution, by the examination of stationary points on the potential surface. Such an approach has been used in finding the dynamic buckling load of a

*Received August 3, 1966. This research was supported by the Advanced Research Projects Agency (Project DEFENDER) and was monitored by the U. S. Army Research Office-Durham under Contract DA-31-124-ARO-D-257.

shallow elastic arch [4]. In the dissipative case, the buckling load cannot be determined exactly by the energy method, but we will show that an adequate upper bound can be obtained. In this method, some use is made of the properties of critical points of a plane, autonomous system of differential equations, ([5], [6], [7]). The system under study (see Eqs. (10a, b) below) is of the Liénard type ([7, p. 267]) which has received much attention, although apparently not for the type of physical problem that is considered here.

2. A simple plane truss model. In Fig. 1, a symmetrical linkage of two massless straight bars, each of undeformed length $a \sec \theta_0$ and cross-sectional area A, is shown attached by frictionless pins to a mass M and to supports. The load P is applied to the mass M at time $t = 0+$ and is held constant thereafter. Gravity is neglected. The assumption $[h(t)/a]^2 \ll 1$ will be made for all t from $t = 0$ to t at a critical value. Hence, the approximations $\theta \doteq h/a$, $\theta_0 \doteq h_0/a$ will be valid. Relevant equations are therefore (see Fig. 1): strain-displacement,

$$\epsilon = \frac{a \sec \theta - a \sec \theta_0}{a \sec \theta_0} = \frac{1}{2a^2}(h^2 - h_0^2); \tag{1}$$

motion, F being the axial force in each bar,

$$2F \sin \theta + P = M \frac{d^2}{dt^2}(h_0 - h); \tag{2}$$

and the constitutive relation for the Voigt material,

$$\sigma = E\epsilon + \eta \frac{d\epsilon}{dt}. \tag{3}$$

It is assumed that the straight bars do not buckle, so that $\sigma = F/A$.

Introduction of the nondimensional nomenclature

$$y = h/h_0\,, \qquad \tau = t(Ah_0^2E/Ma^3)^{1/2}, \qquad p = Pa^3/h_0^3EA,$$
$$\kappa = 2\eta(Ah_0^2/a^3ME)^{1/2} \tag{4}$$

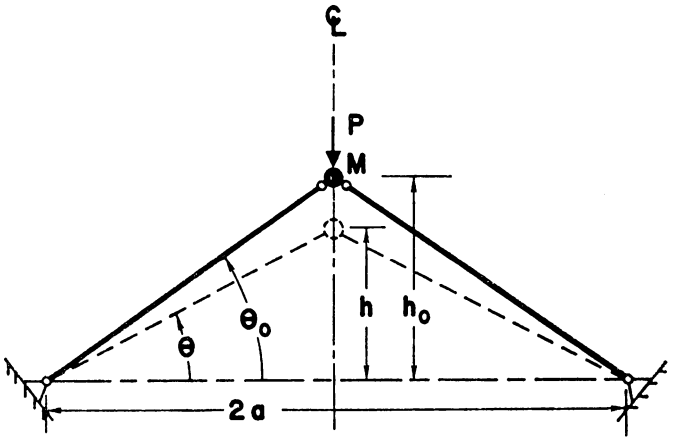

FIG. 1. Geometry of the Plane Truss Model.

enables the writing of Eqs. (1), (2), (3), respectively, as follows for shallow trusses:

$$\epsilon = \frac{h_0^2}{2a^2}(y^2 - 1) \tag{5a}$$

$$\frac{\sigma}{E} = -\frac{h_0^2}{2a^2}\frac{p + \ddot{y}}{y} = \epsilon + \tfrac{1}{2}\kappa\dot{\epsilon} \tag{5b}$$

where $(\dot{}) = d/d\tau$ ( ). Upon substitution from Eq. (5a) into (5b), there is obtained a single equation for $y(\tau)$:

$$\ddot{y} + \kappa y^2\dot{y} + y^3 - y + p = 0, \qquad \tau > 0. \tag{6}$$

The initially undisturbed structure has the initial conditions

$$y(0+) = 1 \quad \text{and} \quad \dot{y}(0+) = 0. \tag{7}$$

The energy integral is obtained from Eq. (6) by multiplying both sides of the equation by $\dot{y}$ and integrating from $\tau = 0$ to an arbitrary τ, while taking into account the initial conditions, Eq. (7). The equation obtained,

$$\frac{\dot{y}^2}{2} + \tfrac{1}{4}(1 - y^2)^2 + p(y - 1) = -\kappa\int_0^\tau y^2\dot{y}^2\, d\tau', \tag{8}$$

represents conservation of energy in nondimensional form for the actual motion $y(\tau)$. That is, K, U and D are, respectively, nondimensional forms of the kinetic energy, total potential energy and total dissipated energy:

$$K = \tfrac{1}{2}\dot{y}^2; \qquad U(y, p) = \tfrac{1}{4}(y^2 - 1)^2 + p(y - 1); \qquad D = \kappa\int_0^\tau y^2\dot{y}^2\, d\tau'. \tag{9}$$

Equation (8) states that $K + U + D = 0$ is an integral of the motion.

By the substitutions $x_1 = y$, $x_2 = \dot{y}$, Eq. (6) can be put into the form of a two-dimensional, real, autonomous nonlinear system for $\tau > 0$:

$$\dot{x}_1 = x_2 \tag{10a}$$

$$\dot{x}_2 = -\kappa x_1^2 x_2 + x_1 - x_1^3 - p \tag{10b}$$

with initial conditions

$$x_1(0) = 1 \quad \text{and} \quad x_2(0) = 0. \tag{10c}$$

Use will be made of the theory of such autonomous systems (see [5], [6], [7]) to determine the qualitative behavior of the solutions describing positive half-characteristics (or semiorbits) in the (x_1, x_2) or $(y, \dot{y})$ phase plane. It is known that critical points for such a system on the phase plane are those points for which the right-hand sides of Eqs. (10a, b) vanish simultaneously. These are defined by

$$\dot{y} = 0 \tag{11a}$$

and the real-valued roots of the equation

$$y^3 - y + p = 0. \tag{11b}$$

The real-valued roots of Eq. (11b) can be expressed explicitly for ranges of the load parameter p in the following way. For $0 \leqq p \leqq \frac{2}{3}(3)^{-1/2}$, let $3\alpha \equiv \sin^{-1}[3(3)^{1/2}p/2]$,

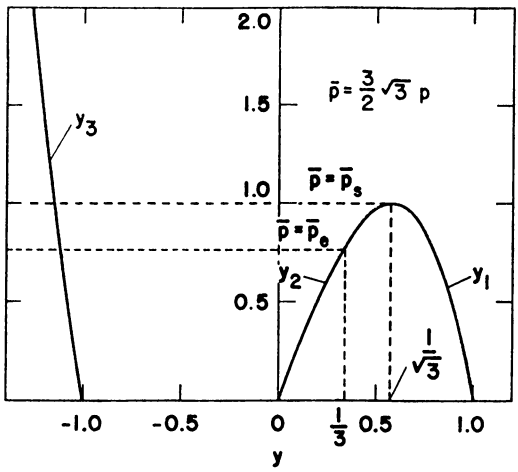

FIG. 2. Critical Points y_i as Function of Load Parameter p.

where $0 \leqq \alpha \leqq \pi/6$. Then the roots are $y = y_i$, $i = 1, 2, 3$, $y_1 \geqq y_2 \geqq 0 > y_3$ (Fig. 2).

$$y_1 = \cos\alpha - \frac{1}{3^{1/2}}\sin\alpha \tag{12a}$$

$$y_2 = \frac{2}{3^{1/2}}\sin\alpha \tag{12b}$$

$$y_3 = -\cos\alpha - \frac{1}{3^{1/2}}\sin\alpha. \tag{12c}$$

At $p = \frac{2}{3}(3)^{-1/2}$, roots $y_1 = y_2 = 1/3^{1/2}$. For $p > \frac{2}{3}(3)^{-1/2}$, there is only one real-valued root. Let $\bar{p} \equiv 3(3)^{1/2}p/2$ and consider $\bar{p} \geqq 1$:

$$y_3 = -\frac{1}{3^{1/2}}[(\bar{p} + (\bar{p}^2 - 1)^{1/2})^{1/3} + (\bar{p} - (\bar{p}^2 - 1)^{1/2})^{1/3}]. \tag{12d}$$

The behavior of solutions to the nonlinear equations (10a, b) in the vicinity of each of the three critical points $x_1 = y_i$, $x_2 = 0$, $i = 1, 2, 3$, is found from examination of the linear perturbed system. Upon substitution of $x_1^L = x_1 - y_1$, $x_2^L = x_2$ into Eqs. (10a, b), and upon linearization with respect to x_k^L, there is obtained the linear system

$$\dot{x}_1^L = x_2^L \tag{13a}$$

$$\dot{x}_2^L = (1 - 3y_i^2)x_1^L - \kappa y_i^2 x_2^L, \qquad i = 1, 2, 3. \tag{13b}$$

The eigenvalue equation ($x_k^L = a_k \exp \lambda\tau$) has roots λ_{ji}, $j = 1, 2$, for each y_i, $i = 1, 2, 3$.

$$\left.\begin{matrix}\lambda_{1i}\\ \lambda_{2i}\end{matrix}\right\} = -\tfrac{1}{2}\kappa y_i^2 \pm (\tfrac{1}{4}\kappa^2 y_i^4 + 1 - 3y_i^2)^{1/2}. \tag{14}$$

For $0 < \bar{p} < 1$, it follows from Eq. (14) and Fig. 2 that $(1 - 3y_1^2) < 0$. This means that the roots λ_{j1} for small κ are conjugate complex with negative real part, while for larger $\kappa(\kappa > 3)$, λ_{j1} are real and $\lambda_{21} < \lambda_{11} < 0$. For small κ, then, y_1 is a spiral point (vortex point or focus) with a clockwise rotation about $x_1 = y_1$, $x_2 = 0$ in the phase plane, while for larger κ, y_1 is a nodal point (improper node). In either case, y_1 is stable both for the linear and the nonlinear systems.

Since $(1 - 3y_3^2) < 0$ for all $p \geqq 0$, similar conclusions are reached for the critical point y_3 ; it is either a spiral point or a nodal point, and it is stable.

For $0 < \bar{p} < 1$, $(1 - 3y_2^2) > 0$; hence, it follows from Eq. (14) that λ_{12} and λ_{22} are both real and $\lambda_{22} < 0 < \lambda_{12}$. Thus, y_2 is a saddle point for all $\kappa \geqq 0$. Further discussion of the saddle point is reserved for Sec. 4 below. For $\bar{p} = 1$, the critical points y_1 and y_2 coalesce; the coalesced critical point is not an isolated critical point and so is not stable.

The pertinent results from well-known theorems on differential equations may be summarized for present purposes as follows. Since the right-hand sides of Eqs. (10a, b) each possess continuous partial derivatives of all orders with respect to x_1 , x_2 , p and κ, then for all real values κ and p there exists a unique solution to Eqs. (10a, b) in every arbitrary bounded domain R in the phase plane containing the initial point (10c). Furthermore, these solutions are continuously differentiable functions of p and κ, and are continuous with respect to small changes in the initial conditions (10c) as well. The asymptotic behavior as $t \to \infty$ of the solutions to Eqs. (10a, b, c), or, equally, of the solutions to Eqs. (6) and (7), is classified by the Poincaré–Bendixson theorem and the Bendixson theorem for the cases of isolated critical points, (see [5, Chapter 16, Theorem 2.1 and 3.1]; also [6, Chapter 10, Theorem 8.1]). These theorems state that the behavior of the characteristic falls into one of the following mutually exclusive categories: the characteristics either approach a critical point asymptotically; or they approach asymptotically a limit characteristic which tends to a critical point; or the characteristic is a periodic orbit that contains only regular points; or the characteristic approaches a periodic orbit (limit cycle) asymptotically.

For $\kappa > 0$, since D (Eq. (9)) is a monotonically increasing function of time, no periodic solutions (periodic orbits or limit cycles) can exist. For $\kappa = 0$, the characteristics in general are periodic orbits enclosing either y_1 only, or both y_1 and y_2 .

The limiting case of quasi-static buckling is readily understood from Fig. 2. If the load P, instead of being suddenly applied at time $t = 0$, is applied as a very slowly increasing function of time, then for sufficiently small values of p the motion will follow a succession of equilibrium states defined by the curve in Fig. 2 labelled y_1 . For $p > \frac{2}{3}(3)^{-1/2}$, however, there is no continuous path of equilibrium states; the critical point y_1 no longer exists. Hence, the quasi-static buckling load is $p = p_s$, where

$$p_s = \tfrac{2}{3}(3)^{-1/2} = 0.385. \tag{15}$$

It follows that, for the case of suddenly applied loading, the dynamic buckling load p_b must approach p_s as κ or η assume sufficiently large values. The motion $y(t)$ is determined in this case by neglecting $\ddot{y}$ in Eq. (6), giving

$$t = \frac{2\eta}{E} \int_{y(t)}^{1} \frac{y^2\, dy}{p + y^3 - y}. \tag{16}$$

From Eq. (16), it is seen that as $t \to \infty$ the motion approaches y_1 for $p < p_s$ and y_3 for $p > p_s$.

The behavior in the quasi-static case would motivate adoption of the following definition for dynamic buckling in the case of finite κ:

Definition 1. Snap-through or buckling will be said to have occurred whenever the motion as described by its characteristic in the phase plane either is not a periodic orbit enclosing y_1 only or does not approach asymptotically either y_1 or a limit cycle around y_1 only.

This definition would allow the decision as to whether snap-through has occurred to be made solely on the basis of the asymptotic behavior in time. The theorems of the Poincaré–Bendixson theory assure us that buckled motion according to Definition 1 would always in its asymptotic behavior include or approach critical points other than y_1 .

In the physical sense, however, the truss would be regarded as having buckled if the amplitude of motion exceeded the amplitude corresponding to y_3 at any time, regardless of whether the asymptotic behavior of the motion satisfied Definition 1. Indeed, it is shown in Sec. 5 below that, for very special but yet physically possible values of the parameters, the truss will have buckled in the physical sense even though the motion is unbuckled according to Definition 1. Consequently, Definition 1, although mathematically satisfactory, is inadequate to distinguish physical snap-through in all cases. The following definition is preferred:

DEFINITION 2. Snap-through or buckling will be said to have occurred whenever the amplitude of motion exceeds the amplitude corresponding to the saddle point y_2 at any time.

The dynamic buckling load p_b is defined to be the largest value such that, for all $p < p_b$, buckling according to Definition 2 does not occur.

3. Energy integral method. For the limiting elastic case, $\kappa = 0$, Eq. (8) can be used to determine p_b without first obtaining $y(\tau)$. It is seen from Eq. (9) that the equation $\partial U/\partial y = 0$ is equivalent to Eq. (11b), so that the three roots y_i are also the values which make $U(y, p)$ stationary in y for fixed p. Figure 3 shows, however, that y_1 is a local minimum and y_2 a local maximum for U. Since $K \geqq 0$, then $U \leqq 0$ is a necessary condition on the motion, and hence no buckling is possible unless $U(y_2 , p) \leqq 0$.

On the other hand, if $U(y_2 , p) < 0$, it is seen from Fig. 3 that there is

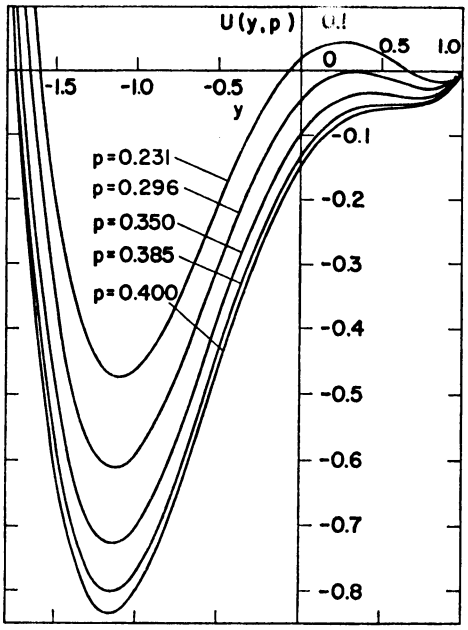

FIG. 3. Total Potential Energy U as Function of y.

some $y = y_p$, $-\infty < y_p < y_3 < -1$, for which $U(y, p) < 0$ on $y_p < y < 1$, and $U(y_p, p) = 0$. On $y_p < y < 1$, therefore, K does not vanish and $\dot{y}$ does not change sign. Let $x_i = x_i^{(1)}(\tau)$ satisfy Eqs. (10a, b) for $0 < \tau < \tau_p$, and satisfy Eqs. (10c), and let $x_1^{(1)}(\tau_p) = y_p$, $x_2^{(1)}(\tau_p) = 0$. Then, for $\tau_p \leqq \tau \leqq 2\tau_p$, $x_1 = x_1^{(1)}(2\tau_p - \tau)$, $x_2 = -x_2^{(1)}(2\tau_p - \tau)$ is the extended solution, and so forth. The solution to Eqs. (10a, b) is therefore periodic with period $2\tau_p$, and the characteristic is a periodic orbit in the phase plane enclosing both y_1 and y_3 . Buckling occurs, then, if $U(y_2, p) < 0$.

Therefore, $U(y_2, p) = 0$ is the necessary and sufficient condition to determine the unique dynamic buckling load p_b . In place of the two conditions $U(y, p_b) = 0$ and $\partial U(y, p_b)/\partial y = 0$, an equivalent single condition is found. Let the function $p(y)$ be defined by the equation $U(y, p(y)) = 0$. The buckling condition is then $dp/dy = 0$. From Eq. (9), the buckling condition is (since $y_2 \neq 1$)

$$\tfrac{1}{4}(y_2 + 1)(y_2^2 - 1) + p_b = 0.$$

Since y_2 and p_b also satisfy Eq. (11b), then by eliminating p_b ,

$$\tfrac{1}{4}(y_2 + 1) = y_2 \quad \text{or} \quad y_2 = 1/3. \tag{17}$$

Substitution of y_2 into Eq. (11b) gives the elastic dynamic buckling load, $p_b = p_e$:

$$p_e = 8/27 = 0.296. \tag{18}$$

For the viscoelastic case, $\kappa > 0$, we have $U < 0$ for $\tau > 0$, since $K \geqq 0$ and $D > 0$. As stated above, if $p < 0.385$, then the potential $U(y, p)$ is stationary at three distinct points $y = y_i$. It is shown in the following section that for each $\kappa > 0$ there is a unique value p_b with the following properties. When $p = p_b$, the local maximum (Fig. 3) of the potential curve at $y = y_2$ can just be reached asymptotically at infinite time. Since $\dot{y} = 0$ at the maximum, then $K = 0$ and $U = -D$ at the maximum. When $p < p_b$, the variation of U during deformation of the structure is restricted to a trough-shaped neighborhood about the minimum at $y = y_1$. Due to strictly increasing energy dissipation, the value of U oscillates about this minimum and approaches it as a limit. When $p > p_b$, the maximum of the potential curve is reached and passed over; in this case, the truss deforms towards the buckled equilibrium position at $y = y_3$.

Thus p_b satisfied the definition of the dynamic buckling load as given above. In the elastic case, p_b is the smallest load for which the local maximum value of U is nonpositive. In the viscoelastic case, the value of load necessary in order to just pass over the local maximum of the potential depends on the viscosity factor κ. The functional dependence of p_b on κ is expressed by the continuous function $p_b = p_b(\kappa)$ for $\kappa \geqq 0$. When $p \geqq 0.385$, the local maximum of the potential curve no longer exists (Fig. 3). The structure must then deform to a buckled position. Therefore, this value, $p = p_e$ (Eq. 15), is an upper bound on $p_b(\kappa)$ for all κ.

4. Phase plane analysis. For $\kappa > 0$, the value of D, Eq. (9), depends upon the solution $y(\tau)$ to Eq. (6). If $y(\tau)$ is unknown, the energy integral method will not yield an exact value for the dynamic buckling load, as it did in Eq. (18) for $\kappa = 0$. However, the method can be used without solving Eq. (6) to determine approximations to p_b .

First, τ will be replaced by y as independent variable. Since for $p > 0$, $\dot{y}(0+) = 0$ but $\ddot{y}(0+) < 0$, then $\dot{y}(\tau) < 0$ in some right-hand neighborhood of the point $\tau = 0$ in the τ axis. Then there exists some τ_p , $0 < \tau_p \leqq \infty$, for which $\dot{y}(\tau) < 0$ for τ in the range $0 < \tau < \tau_p$, and $\dot{y}(\tau_p) = 0$. With the definition $y_p \equiv y(\tau_p)$, the function $y(\tau)$,

defined by

$$y(\tau) = 1 + \int_0^\tau \dot{y}(\tau')\, d\tau',$$

is consequently monotone decreasing in $0 < \tau < \tau_p$, and there exists a single-valued, continuously differentiable and monotone decreasing inverse function $\tau = g(y)$ which is defined on the interval $y_p < y < 1$ with $g(y_p) = \tau_p$ and $g(1) = 0$. The single-valued and continuously differentiable function $\dot{y} = \phi(y)$ then has the following properties on $y_p < y < 1$,

$$\phi(y) \equiv \dot{y}(g(y)) \tag{19a}$$

$$\phi(y) < 0 \tag{19b}$$

$$\phi \frac{dg}{dy} = 1 \tag{19c}$$

and, at the ends of the interval,

$$\phi(y_p) = \phi(1) = 0. \tag{19d}$$

With use of Eq. (19c), the integral in Eq. (9) for D can be transformed on $0 < \tau < \tau_p$ by substitution of the integration variable y' for τ':

$$D = \kappa \int_0^\tau y^2(\tau')\dot{y}^2(\tau')\, d\tau' = \kappa \int_1^y y'^2\phi(y')\, dy'.$$

Equation (8) can therefore be written as

$$p(1 - y) = \tfrac{1}{2}[\phi(y)]^2 + \tfrac{1}{4}(1 - y^2)^2 + \kappa \int_y^1 y'^2[-\phi(y')]\, dy' \tag{20}$$

for all y in $y_p < y < 1$. Also, in view of Eq. (19d),

$$p(1 - y_p) = \tfrac{1}{4}(1 - y_p^2)^2 + \kappa \int_{y_p}^1 y^2[-\phi(y)]\, dy. \tag{21}$$

For given positive values of p and κ, if y_p has been determined, and if an upper bound can be found for $-\phi(y)$ on $y_p < y < 1$, then it is evident that Eq. (21) will yield an inequality that will give an upper bound on p. One upper bound on $(-\phi)$ can be found immediately from Eq. (20). We note that the last two terms on the right-hand side are nonnegative; therefore,

$$p(1 - y) \geqq \tfrac{1}{2}[\phi(y)]^2$$

and so, for $y_p \leqq y \leqq 1$,

$$-\phi(y) \leqq [2p(1 - y)]^{1/2}. \tag{22}$$

It will be shown now that, for $p = p_b$, we have $y_p = y_2$, where y_2 is the known function of p_b given by Eq. (12b). This statement has already been shown to be true for $\kappa = 0$.

For positive κ, we examine on the phase plane the characteristic of the solution $x_1(\tau)$, $x_2(\tau)$ for $\tau > 0$ and, in particular, the portion of the characteristic for $0 < \tau \leqq \tau_p$, in which time interval the solution can be represented by the curve $x_1 = y$, $x_2 = \phi(y)$ according to the preceding discussion. If the function $f(x_1, x_2)$ is defined on the entire phase plane as

$$f(x_1, x_2) \equiv \kappa x_1^2 x_2 + \frac{\partial}{\partial x} U(x_1, p) = \kappa x_1^2 x_2 + x_1^3 - x_1 + p, \tag{23}$$

then Eq. (10b) is simply $\dot{x}_2 = -f(x_1, x_2)$. The curve in the phase plane along which $f = 0$ is given analytically by

$$x_2 = -\frac{x_1^3 - x_1 + p}{\kappa x_1^2}, \tag{24}$$

and the several branches of this curve are shown by the dashed lines in Fig. 4. The branches of the curve $f = 0$ divide the phase plane into domains in which either $f > 0$ or $f < 0$. The intersections of these branches with the line $x_2 = 0$ are the roots of $\partial U/\partial x_1$, and these roots are the three critical points $x_1 = y_i$, $i = 1, 2, 3$.

The tangent slope angle θ of the solution characteristic is given by

$$\tan\theta = \frac{\dot{x}_2}{\dot{x}_1} = \frac{\dot{x}_2}{x_2} = -\frac{f(x_1, x_2)}{x_2}. \tag{25}$$

If $x_2 \neq 0$, the characteristic of the solution has a horizontal tangent at its intersections with the curve $f = 0$. These intersections are then stationary values—maxima or minima—for the characteristic. The algebraic sign of $\dot{x}_2$ is opposite to the algebraic sign of f in the domains between intersections, as is demonstrated by the characteristic illustrated in Fig. 4.

In particular, for the portion of the solution characteristic represented for $0 < \tau < \tau_p$ by $x_1 = y$, $x_2 = \phi(y)$, one can write $f = -x_2\dot{x}_2/\dot{x}_1$, and so from Eqs. (19) and (23):

$$\phi\frac{d\phi}{dy} = \ddot{y} = -f(y, \dot{y}), \qquad y_p \leqq y \leqq 1. \tag{26}$$

For $\phi < 0$, $d\phi/dy$ has the same algebraic sign as f and vanishes whenever $\phi(y)$ intersects a branch of the curve $f = 0$.

We now consider in the phase plane, for any fixed, positive value of κ, the one-parameter family of solution curves $\phi(y; p, \kappa)$ with positive p as the parameter and with $y_p \leqq y \leqq 1$. Theorem 1A and Collary in Appendix A show that away from the initial point $y = 1$, curves of this family do not intersect either themselves or one another, and

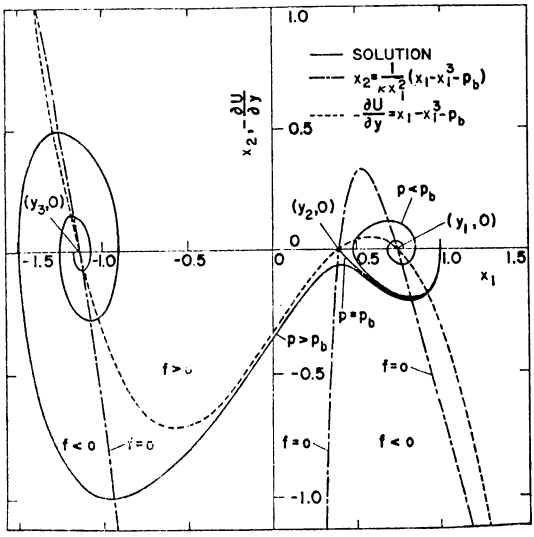

FIG. 4. Phase Plane for $\kappa = 0.5$, ($p_b = 0.334$).

moreover, the curve $x_2 = \phi(x_1 ; p', \kappa)$ lies everywhere below the curve $x_2 = \phi(x_1 ; p, \kappa)$ if p' is greater than p. It then follows, as is illustrated by the solid curves in Fig. 4, that curves of this family must behave in the following mutually exclusive ways:

(a) the curve intersects the $x_2 = 0$ line at $x_1 = y_p$ for $y_2 < y_p < y_1$;
(b) $y_p = y_2$;
(c) the curve intersects the branch of the curve $f = 0$ at a point (x_{1p} , x_{2p}), where $0 < x_{1p} < y_2$ and $x_{2p} < 0$.

From Theorem 2A, Appendix A, we know that in case (a) above, y_p is a continuous, monotonically decreasing function of p. We have seen that y_2 is a continuous, monotonically increasing function of p, and so there exists a finite $p = p_b$ at which

$$y_p = y_2(p_b) \equiv y_b . \tag{27}$$

There cannot be more than one such value p_b , for otherwise there will be more than one y_b , and this would violate the nonintersection property. Hence, there is one and only one value p_b corresponding to case (b).

For case (c), x_{1p} is a continuous, monotonically increasing function of p that approaches $x_{1p} = y_b$ in the limits as p tends to p_b from larger values. Hence, p_b is the least upper bound for p in case (a) and the greatest lower bound for p in case (c). In case (c), it is evident from the geometrical considerations that $y_p < y_3$, and that the truss will in consequence have at some time a deflection greater than that corresponding to y_3 . Conversely, for case (a), the deflection of the truss can never exceed that corresponding to y_b . Therefore, p_b is the dynamic buckling load in accordance with Definition 2 above, and it does represent the load above which snap-through will occur in the physical problem.

5. Application of energy integral method for $\nu > 0$. We consider now the determination of approximations to the function $p_b(\kappa)$ by the use of an energy integral method. For all $\kappa \geqq 0$, let $[-\phi_u(y; p_b , \kappa)]$ be any integrable function which is known to be greater than or equal to the solution $[-\phi(y; p_b , \kappa)]$ on $y_b \leqq y \leqq 1$ and for which $[-\kappa\phi_u]$, as a function of κ for each y and p_b , is monotonically increasing with κ. Equation (21) can then be written as an inequality:

$$p_b(1 - y_b) \leqq \tfrac{1}{4}(1 - y_b^2)^2 + \kappa \int_{y_b}^{1} y^2[-\phi_u(y; p_b , \kappa)]\, dy. \tag{28}$$

Since y_b and p_b satisfy Eq. (8b), then

$$p_b = y_b - y_b^3 . \tag{29}$$

Substitution from Eq. (29) into Eq. (28) gives

$$\tfrac{1}{4}(1 - y_b^2)(1 - y_b)(3y_b - 1) \leqq \kappa \int_{y_b}^{1} y^2[-\phi_u(y; y_b - y_b^3 , \kappa)]\, dy. \tag{30}$$

For each value of y_b in the known range $\frac{1}{3} \leqq y_b \leqq 1/3^{1/2}$, let κ^* be the unique root of the equation

$$\tfrac{1}{4}(1 - y_b^2)(1 - y_b)(3y_b - 1) = \kappa^* \int_{y_b}^{1} y^2[-\phi_u(y; y_b - y_b^3 , \kappa^*)]\, dy. \tag{31}$$

With p_b given by Eq. (29), inequality (30) then implies that

$$\kappa \geqq \kappa^*. \tag{32}$$

Thus, inequality (30) can be used to determine a lower bound κ^* on κ for each p_b, or, conversely, an upper bound on p_b for each κ. We note that for $y_b = \frac{1}{3}$, $\kappa^* = 0$, and so $\kappa^* = \kappa$ for the elastic case previously discussed, (Eq. (17)).

As an example of application of this method, the upper bound of inequality (22) is selected; we take

$$-\phi_u = [2p_b(1 - y)]^{1/2} = [2y_b(1 - y_b^2)]^{1/2}(1 - y)^{1/2}. \tag{33}$$

Since

$$\int_{y_b}^{1} y^2(1 - y)^{1/2}\, dy = \tfrac{2}{105}(8 + 12y_b + 15y_b^2)(1 - y_b)^{3/2}$$

then Eq. (31) becomes

$$\kappa^* = \frac{105}{8} \frac{(1 + y_b)^{1/2}(3y_b - 1)}{(2y_b)^{1/2}(8 + 12y_b + 15y_b^2)}. \tag{34}$$

With p_b and κ^* computed parametrically from Eqs. (29) and (34), the upper bound on $p_b(\kappa)$ that is obtained is shown by a dashed line on Fig. 5. This is compared to the numerical solution of Eq. (6) that is obtained in the following section. The bound for $p_b(\kappa)$ for values of κ not close to $\kappa = 0$ is quite high because the approximation function ϕ_u in Eq. (33) does not satisfy the condition that the solution must satisfy: $\phi_u = 0$ at $y = y_b$. Furthermore, this ϕ_u is independent of κ, and in regard to this point, it can be observed with the aid of Fig. 4 that, for $p \leqq p_b$, the solution ϕ is bounded as

$$[-\phi(y; p, \kappa)] < p/\kappa \quad \text{for} \quad y_b \leqq y \leqq 1. \tag{35}$$

A better approximation to $p_b(\kappa)$ is obtained by choosing a trial function for ϕ which does vanish properly at both $y = 1$ and $y = y_b$. At $y = y_b$, which is the saddle point y_2, it is known that the characteristic that enters this point is tangent there to the separatrix. The tangent lines to the separatrix at y_2 have the following equations on the phase plane:

$$x_2 = \lambda_{22}(x_1 - y_2) \quad \text{and} \quad x_2 = \lambda_{12}(x_1 - y_2) \tag{36}$$

where the λ_{j2} are given by Eq. (14) above. Hence, it follows that, for small positive values of $y - y_b$,

$$\phi(y; p, \kappa) \doteq \lambda_{22}(y - y_b). \tag{37}$$

Equation (37) can also be obtained from Eq. (26):

$$\frac{d\phi}{dy} = -\frac{f(y, \phi)}{\phi} = -\kappa y^2 - \frac{y^3 - y + p}{\phi}.$$

In taking the limit as $y \to y_b$, the last expression on the right is evaluated by L'Hospital's rule, leading to a quadratic equation for the limit value of $d\phi/dy$ (cf. Eq. 16A below). Therefore, the trial function should have the following limiting properties:

$$\lim_{y \to 1} \frac{\phi(y; p, \kappa)}{(1 - y)^{1/2}} = -(2p)^{1/2} \tag{38a}$$

$$\lim_{y \to y_b} \frac{\phi(y; p, \kappa)}{y - y_b} = \lambda_{22}\,. \tag{38b}$$

The following trial function

$$-\phi = (2p)^{1/2}(1 - y_b)^{-1}(1 - y)^{1/2}(y - y_b) - [(2p)^{1/2}(1 - y_b)^{-3/2} + (1 - y_b)^{-1}\lambda_{22}](1 - y)(y - y_b) \tag{39}$$

does satisfy Eqs. (38a, b) as well as Eq. (22). It cannot be proven to be an upper bound ϕ_u, but it is quite close to being one. If the right-hand side is substituted for $-\phi_u$ in Eq. (31), the following cubic equation is derived for κ^*:

$$2BC\kappa^{*3} + (B^2 - C^2D - 2AC)\kappa^{*2} - 2AB\kappa^* + A^2 = 0 \tag{40}$$

where

$$A = \tfrac{1}{4}(1 - y_b)(3y_b - 1),$$
$$B = \tfrac{1}{1260}[2y_b(1 + y_b)]^{1/2}(17y_b + 44y_b + 65),$$
$$C = \tfrac{1}{120}y_b^2(3y_b^2 + 4y_b + 3),$$

and

$$D = \frac{4}{y_b^4}(1 - 3y_b^2).$$

Equations (29) and (40) are again parametric equations for p_b and κ^* with y_b as a parameter. This approximate solution of p_b plotted against κ is shown in Fig. 5 by a dotted line, and it is seen to lie close to the exact solution and always above it.

This same procedure can be used to derive lower bound approximations to $p_b(\kappa)$ by using suitable functions $-\phi_L$ which are known to be less than $[-\phi(y; p, \kappa)]$. In this regard, it has been shown here that $[-\phi(y; p'', \kappa)]$ for $p'' < p$ and $[-\phi(y; p, \kappa')]$ for $\kappa' > \kappa$ are both functions of the class $[-\phi_L]$.

6. Direct method for $\kappa > 0$. In order to find the exact values of the critical load, Eqs. (6) and (7) are solved numerically by use of the Runge–Kutta–Gill technique [8]. By comparing the numerical solution of p_b with the known solution of the case $\kappa = 0$, we find that this method can provide good accuracy for our purpose.

The deflection history curves are shown in Fig. 6 for $\kappa = 0.5$. The structure oscillates with decreasing amplitudes due to energy dissipation through the dashpot. For $p < p_b$, the oscillation dies out and approaches a limiting frame height y_1 as $\tau \to \infty$. As the load increases, the truss vibrates with decreasing frequency. At $p = p_b$, the height of the truss approaches a limiting value y_2 asymptotically without vibration. For $p > p_b$, the truss first deforms to a snapped position and then vibrates with decreasing amplitudes.

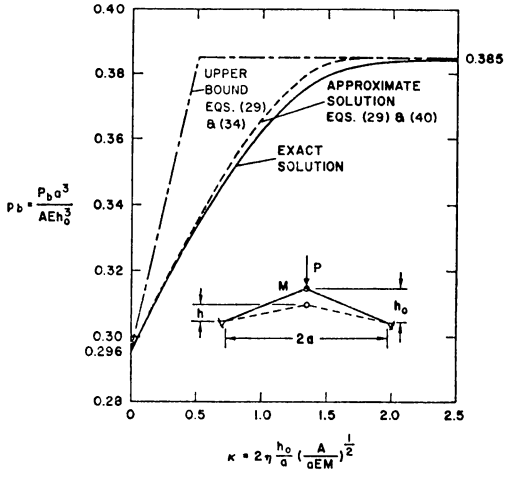

FIG. 5. Dynamic Buckling Load p_b vs. Viscosity Factor κ.

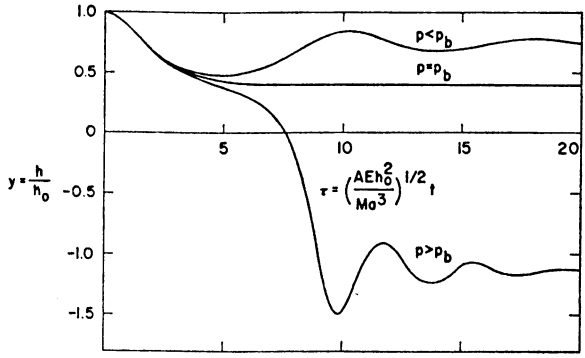

FIG. 6. Deflection Histories for $\kappa = 0.5$, ($p_b = 0.334$).

For most values at κ, if $p > p_b$, the position of the truss will approach y_3 as $\tau \to \infty$. However, when the value of κ is very small ($\kappa < 0.01385$), there are some ranges of κ within which the truss will approach $y = y_1$ as $\tau \to \infty$. This behavior can easily be visualized from the potential curves (Fig. 3). During the oscillation of the truss, the value of the potential energy changes with y along the curves shown in Fig. 3. For sufficiently small values of κ, the potential energy can pass over the local maximum at $y = y_2$ back and forth several times, and then finally approaches the local minimum of either y_1 or y_3 depending on the total dissipated energy D during the oscillation. The narrow regions in $p - \kappa$ diagram for $y(\infty) = y_1$ are shown in Fig. 7 and Table 1. When $p > 0.385$, the local maximum of the potential curve disappears; hence, the truss always stops at a height y_3. From Fig. 7, we conclude that for either $\kappa = 0$ or $\kappa > 0.01385$ the two definitions of dynamic buckling given in Sec. 2 are actually equivalent; otherwise, they need not be equivalent.

Note that the nondimensional height at infinite time depends only on the load parameter p but not on the viscosity factor κ on account of the delayed elastic characteristic of Voigt solids. In the problem considered in this paper, it is possible to define the dynamic buckling load according to the definitions of Sec. 2. On the other hand, these definitions of dynamic buckling cannot be applied to all viscoelastic structures. For example, the structure made of the Maxwell solids can flow indefinitely, and it always deforms to a snapped-through position at large time.

The nondimensional dynamic buckling load p_b is plotted against the viscosity factor κ in Fig. 5. It is found that the viscoelastic buckling load is higher than the elastic buckling load. In Theorem 2A, Appendix A, we have proved that the value of y_p for the

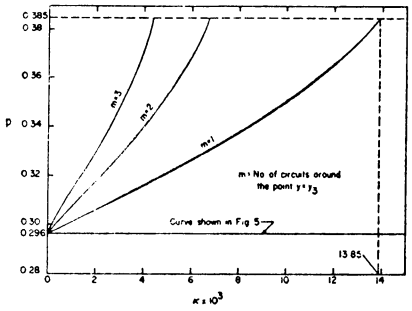

FIG. 7. Regions for $y(\infty) = y_1$ in $p - \kappa$ Diagram.

TABLE 1. *Upper and Lower Limits of Regions of Fig. 7.*

p	$\kappa \times 10^3$					
	$m = 1$		$m = 2$		$m = 3$	
	upper	lower	upper	lower	upper	lower
0.31	2.832	2.747	1.284	1.265	0.774	0.766
0.33	6.696	6.572	3.203	3.174	2.048	2.035
0.35	9.908	9.813	4.804	4.782	3.110	3.101
0.37	12.510	12.475	6.101	6.094	3.973	3.969

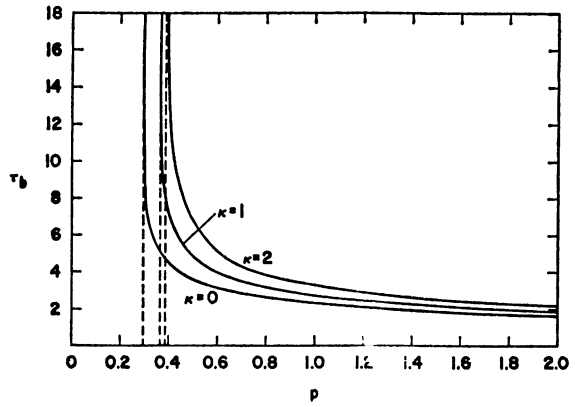

FIG. 8. Nondimensional Time τ_b to Reach the Buckling Height.

viscoelastic case is higher than that of the corresponding elastic case as a result of energy dissipation during deformation. Thus, the possibility of buckling in the viscoelastic case is reduced. As already mentioned in Sec. 2, when the value of κ is very large, the motion of the structure becomes extremely slow and the dynamic buckling load approaches the quasi-static value $p_s = 0.385$.

The nondimensional critical time τ_b for $p > p_b$ can be defined as the smallest time required to reach the height y_2 . This critical time is shown in Fig. 8 for various values of p and κ. At $p = p_b$, the critical time is infinite; as p/p_b becomes large, the critical time approaches zero.

7. Conclusions. The principal conclusions are the following:

(1) The physical meaning of dynamic buckling is that the maximum amplitude of the motion in time, when considered as a function of the applied load, increases in a discontinuous fashion at a particular load, the dynamic buckling load. For larger loads, the structure thus will during its motion deform to a snapped-through position at least temporarily. The saddle point criterion for dynamic buckling (Definition 2) is shown to predict the unique value of the buckling load in all cases. For small values of the viscosity factor, however, an alternate criterion, which looks only at asymptotic behavior in time (Definition 1), will predict no buckling at certain larger loads. At these loads,

snap-through will have occurred in the motion only during finite time, while the structure tends towards an unbuckled equilibrium position for large time. Although it is not the case for the considered structural model, other structures could exhibit such a phenomenon for a continuous range at loads above the dynamic buckling load. It is considered, therefore, that dynamic buckling criteria based upon the asymptotic character of the motion is not satisfactory for dissipative structures.

(2) For a Voigt material, the dynamic buckling load has been shown to lie between the dynamic buckling load for the elastic material as the lower limit and the quasi-static buckling load as the upper limit. The quasi-static buckling load is found from the viscoelastic theory to be equal to the dynamic buckling load in the limit of infinite viscosity.

(3) The energy integral method for prediction of dynamic buckling loads, which has been very useful for elastic structures, is extended to the present viscoelastic structure. The extended method is shown to be useful for computation of bounds on the dynamic buckling load for the viscoelastic case with the use of trial functions that bound or approximate solutions to the differential equations.

Acknowledgement. The authors wish to express thanks to Mrs. M. Bryant for programming, Mr. W. N. Huang for preparation of figures, and Mrs. A. Brick for preparation of manuscript.

References

1. R. Mises, *Über die Stabilitätsprobleme der Elastizitätstheorie*, Z. Angew. Math. Mech. **3**, 406 (1923)
2. J. Hult, *Oil canning problems in creep*, Creep in Structures, (Ed. N. J. Hoff), Academic Press, New York, 1962, p. 161
3. N. C. Huang, *Nonlinear creep buckling of some simple structures*, IRPA Report 66-80 prepared for the U. S. Army Research Office-Durham under Contract DA-31-124-ARO-D-257 University of California at San Diego, La Jolla, California, May, 1966
4. N. J. Hoff and V. G. Bruce, *Dynamic analysis of the buckling of laterally loaded arches*, J. Math. Phys. **32**, 276 (1954)
5. E. A. Coddington and N. Levinson, *Theory of ordinary differential equations*, McGraw-Hill, New York, 1955; in particular, Chapters 15 and 16
6. W. Hurewicz, *Lectures on ordinary differential equations*, second printing, M.I.T., Technology Press, Wiley, New York; in particular, Chapters 4 and 5
7. S. Lefschetz, *Differential equations-Geometric theory*, Second Ed., Interscience, New York, 1963
8. A. Ralston and H. Wilf, *Mathematical methods for digital computers*, Wiley, New York, 1960, p. 110.

Appendix A

Theorems on $\phi(y; p, \kappa)$. With regard to the family of curves $x_1 = y$, $x_2 = \phi(y; p, \kappa)$ in the x_1 , x_2 phase plane, as described in Sec. 4 above, the following theorem is proven.

Theorem 1A. *Two curves of the family $\phi(y; p, \kappa)$ for distinct values of p or distinct values of κ do not intersect one another for $\phi < 0$.*

Equation (22) shows that for $(1 - y)$ nonnegative but sufficiently small, ϕ is approximately given by

$$-\phi \doteq [2p(1 - y)]^{1/2}. \tag{1A}$$

Therefore, if $p' > p$, the curve $\phi(y; p', \kappa)$ lies below the curve $\phi(y; p, \kappa)$ for y near 1. If substitution is made from Eq. (1A) into Eq. (20), the following expression is also obtained for small, negative values of $(1 - y)$:

$$\phi^2 \doteq 2p(1 - y) - \frac{4\kappa}{3}(2p)^{1/2}(1 - y)^{3/2}. \tag{2A}$$

If $\kappa' > \kappa$, it is seen from Eq. (2A) that the curve $\phi(y; p, \kappa')$ lies above the curve $\phi(y; p, \kappa)$ for y near 1.

Let it now be assumed that these curves have a first intersection for some $x_1 = x_1^*$, $x_2 = x_2^*$ with $x_1^* < 1$ and $x_2^* < 0$. If $\theta_{p'}$ and θ_p are tangent slope angles corresponding to p' and p, respectively, for the same value of κ, Eqs. (23) and (25) show that

$$\tan \theta_{p'} - \tan \theta_p = -(p' - p)/x_2^*. \tag{3A}$$

If $p' > p$, then $\tan \theta_{p'} > \tan \theta_p$. If we take the $-x_1$ direction as $\theta = 0$, then for $x_2 < 0$, $-\pi/2 < \theta < \pi/2$. Hence, $\theta_{p'} > \theta_p$, as is shown on Fig. 1A. However, this condition implies that the curve $\phi(y; p', \kappa)$ lies above the curve $\phi(y; p, \kappa)$ to the immediate right of the point x_1^*, x_2^*, as is illustrated in the figure. This violates the assumption that x_1^*, x_2^* is the first intersection. Hence, these curves cannot intersect.

Similarly, if θ_κ and $\theta_{\kappa'}$ are tangent slope angles corresponding to κ and κ' respectively, for the same value of p, Eqs. (23) and (25) show that

$$\tan \theta_{\kappa'} - \tan \theta_\kappa = x_1^{*2} x_2^* (\kappa' - \kappa). \tag{4A}$$

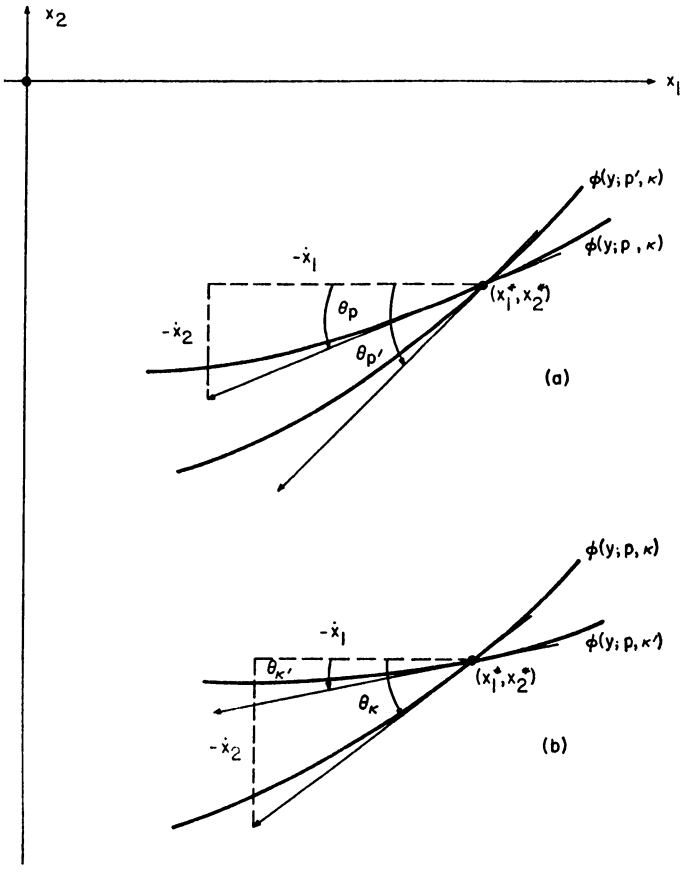

FIG. 1A. Orientation of Curves $\phi(y; p, \kappa)$ at a Supposed First Intersection.

Thus if $\kappa' > \kappa$, $\theta_{\kappa'} < \theta_\kappa$, as is shown on Fig. 1Ab. However, this condition implies that the curve $\phi(y; p, \kappa')$ lies below the curve $\phi(y; p, \kappa)$ to the immediate right of the point x_1^*, x_2^*, as is illustrated in the figure, and this is again a contradiction.

COROLLARY. *For all p', p, κ' and κ such that $p' > p > 0$ and $\kappa' > \kappa \geqq 0$, and for all y such that $\phi < 0$, the following inequalities hold:*

$$-\phi(y; p', \kappa) > -\phi(y; p, \kappa),$$
$$-\phi(y; p, \kappa') < -\phi(y; p, \kappa). \tag{5A}$$

The following theorem concerns the behavior of the characteristics at their intersection with the line $x_2 = 0$, the case that was excluded from the preceding theorem and corollary.

THEOREM 2A. *For $0 < p < p_b$ and $\kappa \geqq 0$, y_p is monotonically decreasing with increasing p for fixed κ and monotonically increasing with increasing κ for fixed p.*

Several preliminary developments are needed before this theorem is proven. First, the following substitutions

$$\eta \equiv y - y_p,$$
$$\xi \equiv y' - y_p, \tag{6A}$$
$$\Phi(\eta) \equiv \phi(y) \quad \text{for} \quad y = \eta + y_p$$

are made in Eq. (20), which then can be written as

$$p(1 - y_p - \eta) = \tfrac{1}{2}\Phi^2 + \tfrac{1}{4}[(1 - y_p - \eta)^2(1 + y_p + \eta)^2] + \kappa\left[\int_{y_p}^{1} y'^2(-\phi)\, dy' - \int_{y_p}^{y} y'^2(-\phi)\, dy'\right]. \tag{7A}$$

The second term on the right-hand side of Eq. (7A) can be expanded in powers of η:

$$\tfrac{1}{4}[(1 - y_p - \eta)^2(1 + y_p + \eta)^2] \doteq \tfrac{1}{4}(1 - y_p^2)^2 - y_p(1 - y_p^2)\eta - \tfrac{1}{2}(1 - 3y_p^2)\eta^2 + y_p\eta^3 + \tfrac{1}{4}\eta^4. \tag{8A}$$

In view of this, and of Eq. (21), Eq. (7A) becomes

$$-p\eta = \tfrac{1}{2}\Phi^2(\eta) - y_p(1 - y_p^2)\eta - \tfrac{1}{2}(1 - 3y_p^2)\eta^2 + y_p\eta^3 + \tfrac{1}{4}\eta^4 - \kappa\int_0^\eta [y_p^2 + 2\xi y_p + \xi^2][-\Phi(\xi)]\, d\xi \tag{9A}$$

A solution to Eq. (9A) is sought with the formal representation of $\Phi(\eta)$ by a power series in the variable $\eta^{1/2}$ for $\eta \geqq 0$:

$$-\Phi(\eta) = \sum_{n=1,2,\cdots}^{\infty} A_n \eta^{n/2}, \tag{10A}$$

where the A_n are constants depending upon p, κ and y_p. If A_n is defined to be zero for $n = 0, -1, -2, \cdots$, then

$$\Phi^2(\eta) = \sum_{n=2}^{\infty} \Big(\sum_{i+j=n} A_i A_j\Big)\eta^{n/2}. \tag{11A}$$

Upon substitution from Eqs. (10A) and (11A) into Eq. (9A), there is obtained the equation

$$-p\eta = \frac{1}{2}\sum_{n=2}^{\infty}\Big(\sum_{i+j=n} A_iA_j\Big)\eta^{n/2} - y_p(1-y_p^2)\eta - \tfrac{1}{2}(1-3y_p^2)\eta^2 + y_p\eta^3 + \eta^4 - \kappa\sum_{k=1}^{\infty}\left[\frac{2}{2+k}\,\eta^{(k/2)+1}(y_p^2A_k + 2y_pA_{k-2} + A_{k-4})\right]. \tag{12A}$$

Equation (12A) can hold for some positive range in η only if the coefficient of each power of $\eta^{1/2}$ vanishes. The lowest order terms are of order η:

$$-p\eta = \tfrac{1}{2}A_1^2\eta - y_p(1-y_p^2)\eta$$

which then yields

$$A_1^2 = 2[y_p(1-y_p^2) - p]. \tag{13A}$$

It follows from the discussion of Eq. (11b) that if $y_2 \leqq y_p \leqq y_1$, then A_1^2 is positive in the open interval for y_p and approaches zero as y_p approaches y_2.

The terms of next higher order are of order $\eta^{3/2}$:

$$\tfrac{1}{2}(2A_1A_2)\eta^{3/2} - \kappa\cdot\tfrac{2}{3}y_p^2A_1\eta^{3/2} = 0. \tag{14A}$$

If $A_1 \neq 0$, then

$$A_2 = \tfrac{2}{3}\kappa y_p^2\,. \tag{15A}$$

If $A_1 = 0$, however, then A_2 is not determined by Eq. (14A) but by the terms of order η^2:

$$\tfrac{1}{2}(2A_1A_3 + A_2^2)\eta^2 - \tfrac{1}{2}(1-3y_p^2)\eta^2 - \kappa\cdot\tfrac{1}{2}y_p^2A_2\eta^2 = 0.$$

For $A_1 = 0$, A_2 obeys the equation

$$A_2^2 - \kappa y_p^2A_2 - (1-3y_p^2) = 0. \tag{16A}$$

If $y_p = y_2$, there are two real-valued roots $A_2 = -\lambda_{12}$ and $A_2 = -\lambda_{22}$ that are given by Eq. (14); these represent the directions of the separatrices at the saddle point.

It is straightforward now to prove Theorem (2A) with the use of Eqs. (13A) and (15A), by means of which we can write, upon substitution of Eqs. (13A) and (15A) into Eqs. (10A) and (6A):

$$-\phi(y;p,\kappa) \doteq 2^{1/2}(y_p - y_p^3 - p)^{1/2}(y-y_p)^{1/2} + \tfrac{2}{3}\kappa y_p^2(y-y_p) \tag{17A}$$

for $0 \leq y - y_p \ll 1$. Assume first that $p' > p$. Since it follows directly from Corollary 1A that $y_{p'}$ cannot exceed y_p, it remains only to show that $y_{p'} \neq y_p$. If equality were the case, however, Eq. (17A) gives

$$[-\phi(y;p',\kappa)] - [-\phi(y;p,\kappa)] = 2^{1/2}(y-y_p)^{1/2}[(y_p - y_p^3 - p')^{1/2} - (y_p - y_p^3 - p)^{1/2}] < 0$$

if $y \neq y_p$ and $y_p \neq y_i$. But this contradicts the first inequality (5A). Similarly, it is again a direct consequence of Corollary 1A that y_p for κ' cannot be less than y_p for κ if $\kappa' > \kappa$. If κ' and κ produce the same value of y_p, then Eq. (17a) shows that

$$[-\phi(y;p,\kappa')] - [-\phi(y;p,\kappa)] = \tfrac{2}{3}y_p^2(y-y_p)(\kappa'-\kappa) > 0$$

which contradicts the second inequality (5A).